

## Characterization of seven xyloglucan oligosaccharides containing from seventeen to twenty glycosyl residues<sup>\*,\*\*</sup>

Makoto Hisamatsu<sup>†</sup>, William S. York<sup>‡</sup>, Alan G. Darvill, and Peter Albersheim  
Complex Carbohydrate Research Center, The University of Georgia, 220 Riverbend Road, Athens GA 30602 (U.S.A.)

(Received May 20th, 1991; accepted for publication 28th June, 1991)

### ABSTRACT

The complete primary structures of seven oligosaccharide subunits of the xyloglucan secreted by suspension-cultured *Acer pseudoplatanus* cells were determined. The oligosaccharides, ranging in size from 17 to 20 glycosyl residues, were generated by treatment of the xyloglucan with an *endo*- $\beta$ -(1 $\rightarrow$ 4)-glucanase. The oligosaccharide components of a fraction obtained by Bio-Gel P-2 chromatography of enzyme-treated xyloglucan were further purified by normal-phase h.p.l.c. and then converted to the corresponding oligoglycosyl alditols by reduction with NaBH<sub>4</sub>. The oligoglycosyl alditols, after purification to near homogeneity by reversed-phase h.p.l.c., were structurally characterized by <sup>1</sup>H-n.m.r. spectroscopy, fast-atom bombardment mass spectrometry (f.a.b.-m.s.), and analysis of their glycosyl-residue and glycosyl-linkage compositions. Novel structural elements of xyloglucans were observed in this study, including  $\beta$ -D-xylopyranosyl and  $\alpha$ -L-arabinofuranosyl-(1 $\rightarrow$ 3)- $\beta$ -D-xylopyranosyl sidechains. The results also extend our list of correlations between <sup>1</sup>H-n.m.r. resonances and specific structural features of xyloglucans and thus enhance our ability to determine the structures of xyloglucans from various sources.

### INTRODUCTION

Xyloglucans (XGs) are highly branched polysaccharides that are closely associated with cellulose microfibrils in the primary cell walls of higher plants. XGs are thought to be major load-bearing structures in the primary cell wall that control the rate of cell-wall expansion, thereby regulating plant cell growth<sup>1</sup>. Furthermore, fucose-containing oligosaccharide subunits of XGs have been shown to inhibit the 2,4-D-stimulated elongation of excised pea-stem sections<sup>2,3</sup>, and the release of these oligosaccharides *in vivo* may also regulate plant cell expansion.

XGs are structurally related to cellulose in that the backbone of these polysaccharides consists of  $\beta$ -(1 $\rightarrow$ 4)-linked Glcp residues, about 75% of which are substituted at C-6 with  $\alpha$ -D-Xylp residues<sup>4,5</sup>. Some of the  $\alpha$ -D-Xylp residues are themselves substituted at C-2 with a  $\beta$ -D-Galp residue or with an  $\alpha$ -L-Fucp-(1 $\rightarrow$ 2)- $\beta$ -D-Galp moiety. Often the D-Galp residue is substituted with one or two *O*-acetyl groups<sup>6</sup>. XGs isolated from the cell walls and culture filtrate of suspension-cultured sycamore cells contain ~2% L-Araf

\* Dedicated to Professor David Manners.

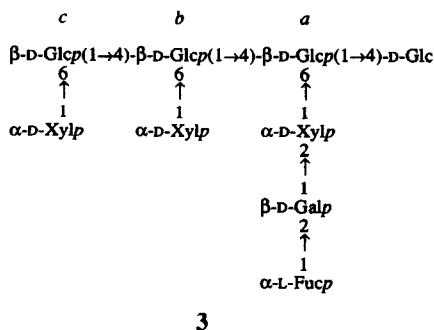
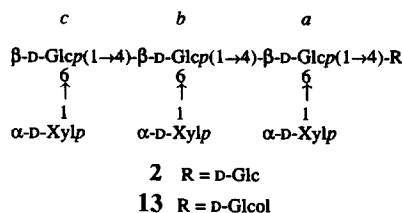
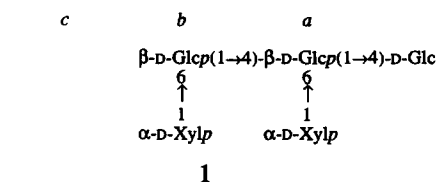
\*\* This is number XXXV of the series entitled The Structure of Plant Cell Walls.

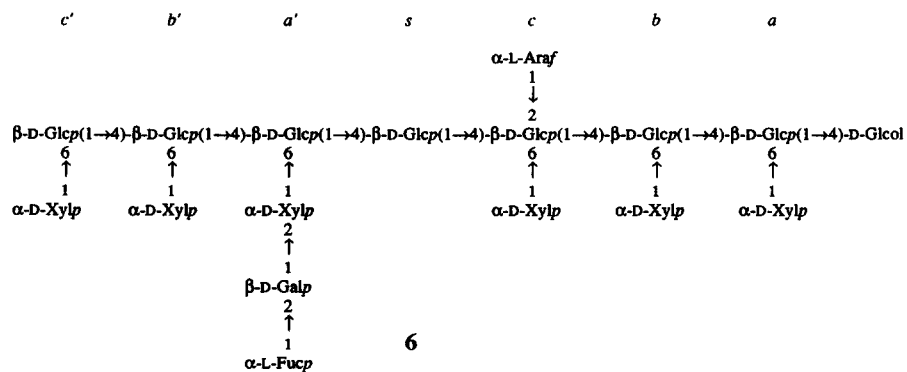
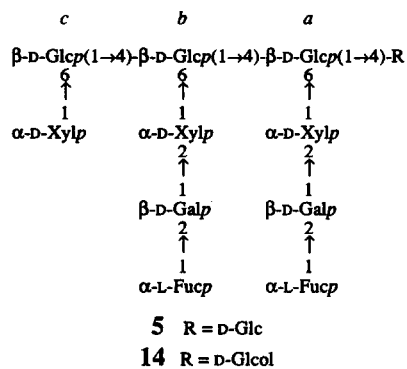
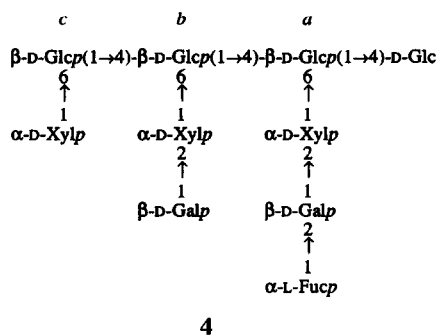
<sup>†</sup> Current address: Faculty of Bioresources, Mie University, 1515 Kamihama, Tsu 514, Japan.

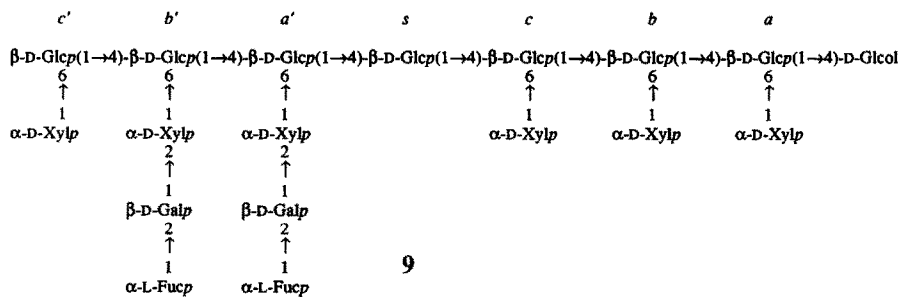
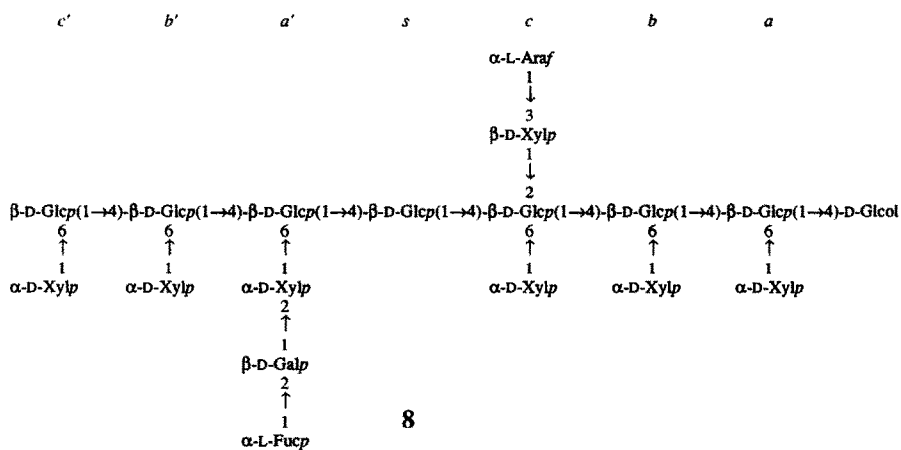
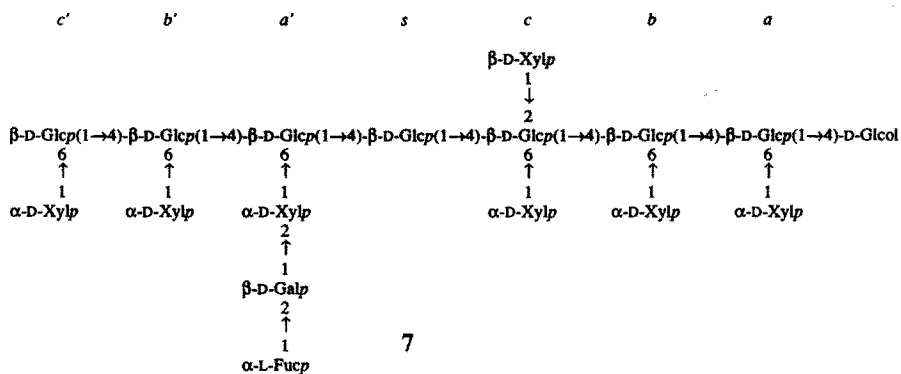
<sup>‡</sup> Author for correspondence.

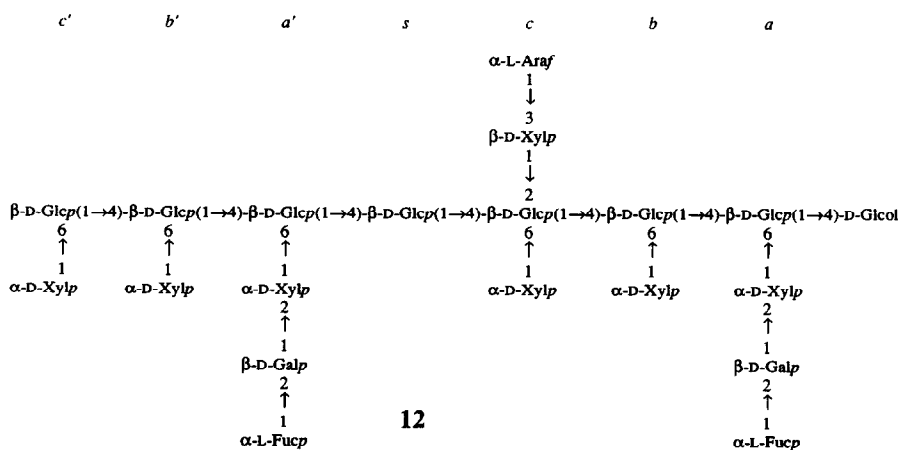
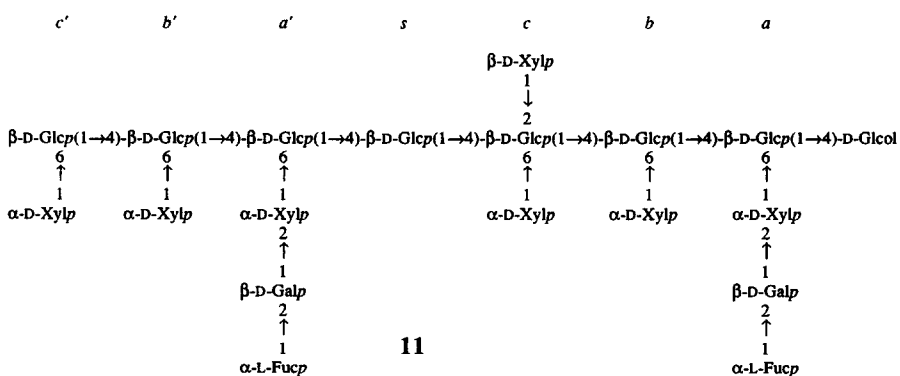
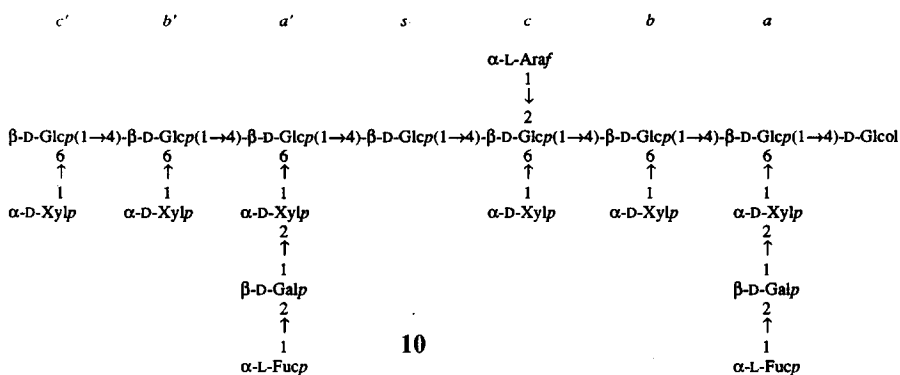
residues, some of which are located at C-2 of 2,4,6-linked Glcp residues<sup>4,7</sup>. We present herein the confirmation of that result and the demonstration that L-Araf residues are also present at C-3 of 3-linked  $\beta$ -D-Xylp residues.

Treatment of XGs with an *endo*-(1 $\rightarrow$ 4)- $\beta$ -D-glucanase isolated from *Trichoderma reesei* cleaves the unbranched (1 $\rightarrow$ 4)-linked  $\beta$ -D-glucosyl residues of the backbone, releasing oligosaccharide subunits<sup>4,5,8</sup> of the polymer. Products obtained when XGs isolated from sycamore cell walls or sycamore extracellular polysaccharides (SEPS) are treated with the *endo*-(1 $\rightarrow$ 4)- $\beta$ -D-glucanase include oligosaccharides 1–5 (Refs. 4, 5, and 8). We define oligosaccharides 1–5 as primary XG subunits because they do not contain any unbranched, 4-linked  $\beta$ -Glcp residues whose glycosidic bonds would normally be cleaved by the purified *endo*-(1 $\rightarrow$ 4)- $\beta$ -D-glucanase. The enzyme also releases larger oligosaccharides that consist of two or more primary subunits and thus include at least one internal unbranched 4-linked  $\beta$ -Glcp residue. These larger oligosaccharides are resistant to cleavage into primary subunits by *endo*-(1 $\rightarrow$ 4)- $\beta$ -D-glucanase due to the presence of additional glycosyl residues that presumably hinder the formation of enzyme–substrate complexes. For example, the arabinose-containing hexadecaglycosyl alditol 6 can be hydrolyzed to primary subunits 2 and 3 by the *endo*-(1 $\rightarrow$ 4)- $\beta$ -D-glucanase only if the Araf residue is first removed<sup>7</sup>.









We now report the isolation and characterization of seven *endo*-(1→4)- $\beta$ -D-glucanase-resistant oligoglycosyl alditols (OAs) (6–12). Oligosaccharides, generated by treating XG with *endo*- $\beta$ -(1→4)-glucanase, were converted to OAs by reduction with  $\text{NaBH}_4$ . The previously characterized<sup>7</sup> arabinose-containing hexadecaglycosyl alditol 6 was included in the study as a reference compound. Six of the OAs that were characterized consist of combinations of primary subunits 2 and 3 substituted with  $\alpha$ -Araf and/or  $\beta$ -Xylp residues that render them totally resistant to cleavage by the *endoglucanase*. Four of the OAs contain  $\beta$ -Xylp residues, which is noteworthy because only  $\alpha$ -linked xylosyl residues had previously been detected in XGs. One of the OAs that was characterized consists of primary subunits 2 and 5, and it is resistant to the *endo*-(1→4)- $\beta$ -D-glucanase due to the unusual nature of subunit 5.

## RESULTS AND DISCUSSION

**Nomenclature.** — Specific glycosyl residues of the OAs described in this paper are designated with superscript lowercase letters (see structures 1–14). This nomenclature reflects the position of each residue *vis à vis* the D-glucitol moiety.  $\beta$ -Glc<sub>p</sub> residues are designated, in order, Glc<sup>a</sup>, Glc<sup>b</sup>, Glc<sup>c</sup>, Glc<sup>s</sup>, Glc<sup>av</sup>, Glc<sup>bv</sup> and Glc<sup>cv</sup>. Thus, Glc<sup>a</sup> is the 4,6-linked  $\beta$ -Glc<sub>p</sub> residue attached to the Glc<sub>ol</sub> moiety, Glc<sup>cv</sup> is the 6-linked  $\beta$ -Glc<sub>p</sub> residue, and Glc<sup>s</sup> is the internal, unbranched 4-linked  $\beta$ -Glc<sub>p</sub> residue that would be susceptible to cleavage by *endoglucanase* in the absence of glycosyl residues at position 2 of Glc<sup>c</sup>. Sidechain residues are referred to using the superscript of the  $\beta$ -Glc<sub>p</sub> residue to which the sidechain is attached.

**Preparation of XG OAs.** — A complex mixture of oligosaccharides was obtained by digesting SEPS XG with *endo*-(1→4)- $\beta$ -D-glucanase. The XG oligosaccharides (600 mg) were separated into molecular size classes by gel-permeation chromatography on Bio-Gel P-2 (Fig. 1). The primary XG subunits (*i.e.*, oligosaccharides containing no

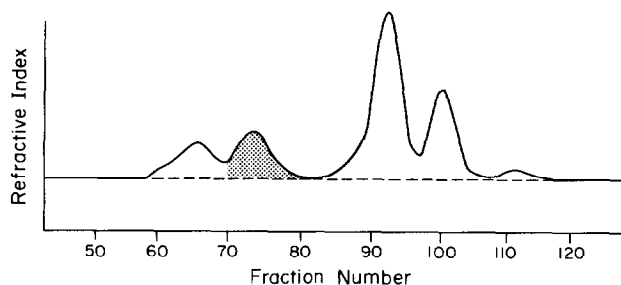


Fig. 1. Bio-Gel P-2 chromatography of 10 mg of the *endo*-(1→4)- $\beta$ -D-glucanase-digested sycamore extracellular XG. Fractions containing oligosaccharides with from 17 to 20 glycosyl residues were pooled as indicated from 10 similar runs (600 mg total XG applied) and combined. The recovery of oligosaccharides in the shaded fractions was estimated colorimetrically (anthrone assay) to be 102 mg.

internal unbranched 4-linked  $\beta$ -Glc<sub>p</sub> residues) in the mixture were eluted from the Bio-Gel column in fractions 80–117 and have been shown<sup>4,5</sup> to consist mostly of compounds 1–5. Fractions 70–79 (shaded in Fig. 1) contained a complex mixture of XG

oligosaccharides with from 17 to 20 glycosyl residues, including the previously characterized<sup>7</sup> 6. Fractions 59–69 contained XG oligosaccharides much larger than compound 6.

The partially purified XG oligosaccharides were separated by a combination of h.p.l.c. techniques. Four fractions (N1–N4) were obtained by h.p.l.c. of P-2 fractions 70–79 on an amino-bonded column (Fig. 2), previously shown<sup>9</sup> to be capable of

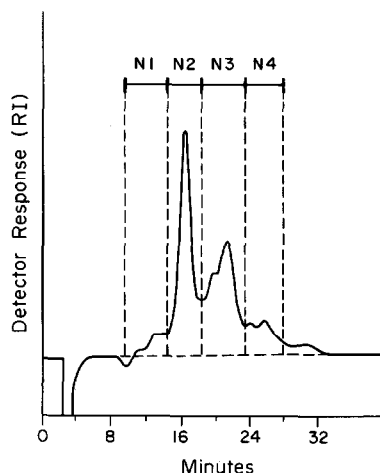


Fig. 2. Normal-phase h.p.l.c. on amino-bonded silica (Dynamax-60A). Oligosaccharides that were partially purified on Bio-Gel P-2 (Fig. 1, shaded fractions) were dissolved in 2.5 mL of water and passed through a Nylon filter (pore size 0.45  $\mu$ m). A 10- $\mu$ L aliquot was injected on the h.p.l.c. column and eluted with 27:23  $\text{CH}_3\text{CN}:\text{H}_2\text{O}$ . The eluates of several preparative runs (50  $\mu$ L injected per run) were pooled as indicated and combined. Total oligosaccharide recoveries were estimated colorimetrically as 4.2 mg (N1), 31.8 mg (N2), 32.4 mg (N3), and 14.4 mg (N4).

separating oligosaccharides based on small differences in their degrees of polymerization. Subsequent analysis (see below) showed that fraction N2 included oligosaccharides (d.p. 17–18) with one fucosyl residue and that fraction N3 included oligosaccharides (d.p. 18–20) with two fucosyl residues. The components of fractions N1 and N4 were not studied further, because only minor amounts of these oligosaccharides were recovered.

The partially purified oligosaccharides in fractions N2 and N3 were converted to the corresponding OAs by reduction with  $\text{NaBH}_4$  in order to simplify their subsequent purification by reversed-phase chromatography. The resulting fractions were designated R2 and R3, respectively. The reduction step was necessary because reversed-phase h.p.l.c. often separates oligosaccharides that differ only in the anomeric configuration of the reducing glucose residue, resulting in two peaks for every oligosaccharide that is applied to the column. In addition, the  $^1\text{H}$ -n.m.r. and negative-ion f.a.b.-m.s. spectra of XG oligoglycosyl alditols are more easily interpreted than those of the corresponding reducing oligosaccharides<sup>5,7</sup>.

The components of R2 and R3 were further purified by reversed-phase h.p.l.c. on octadecylsilyl silica. Efficient separation of each mixture of OAs that was applied to the column required elution with a different ratio of CH<sub>3</sub>OH:H<sub>2</sub>O (Fig. 3). Fractions R2·1

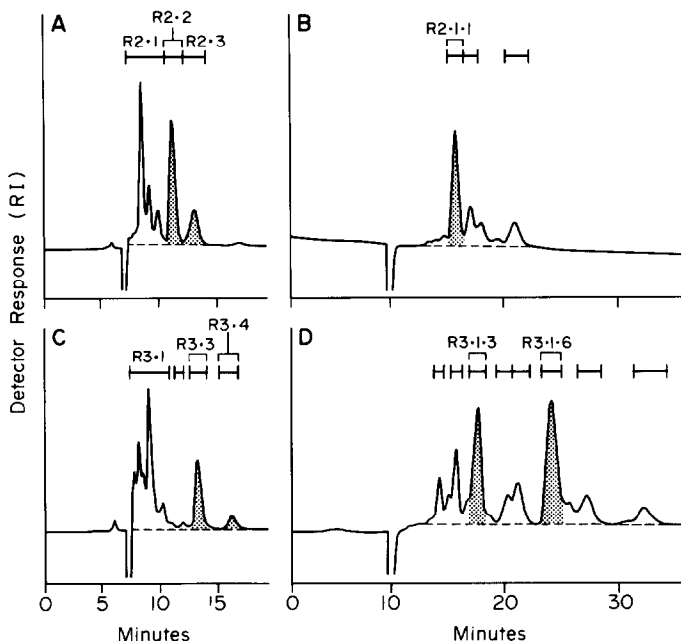


Fig. 3. Reversed-phase h.p.l.c. of oligoglycosyl alditols on a Hibar Lichrosorb RP-18 semipreparative column. Oligosaccharide fractions N2 and N3 (see Fig. 2) were reduced with NaBH<sub>4</sub> to the corresponding oligoglycosyl alditols. The resulting preparations (R2 and R3, respectively) were chromatographed on the RP-18 column. (A) Fraction R2 eluted with 22.5% aqueous MeOH; (B) fraction R2·1 from panel A reappplied and eluted with 21% aqueous MeOH; (C) fraction R3 eluted with 24% aqueous MeOH; (D) fraction R3·1 from panel C reappplied and eluted with 21% aqueous MeOH.

and R3·1, obtained by reversed-phase chromatography of fractions R2 and R3, respectively, were reappplied to the column in order to adequately separate their components (Fig. 3B and 3D). The purity of the OAs contained in fractions R2·1·1, R2·2, R2·3, R3·1·3, R3·1·6, R3·3, and R3·4 was evaluated by 500-MHz <sup>1</sup>H-n.m.r. spectroscopy (Fig. 4). Each fraction except R2·3 contained a >80% pure OA. The mixture of OAs in fraction R2·3 was reappplied to the amino-bonded column and eluted with CH<sub>3</sub>CN:H<sub>2</sub>O (3:2, v/v), yielding fraction R2·3\* (chromatogram not shown). The major component of fraction R2·3\* was an OA that was judged >80% pure by <sup>1</sup>H-n.m.r. spectroscopy (Fig. 4). The remainder of this manuscript described the structural characterization of the purified OAs, recovered in the following yields: **6** in R2·1·1 (4.8 mg); **7** in R2·2 (4.6 mg); **8** in R2·3\* (1.8 mg); **9** in R3·1·3 (3.2 mg); **10** in R3·1·6 (4.8 mg); **11** in R3·3 (5.6 mg); **12** in R3·4 (1.8 mg). These seven OAs thus represent a total of approximately 5 to 10% of the structure of SEPS XG (taking into account losses incurred during purification).



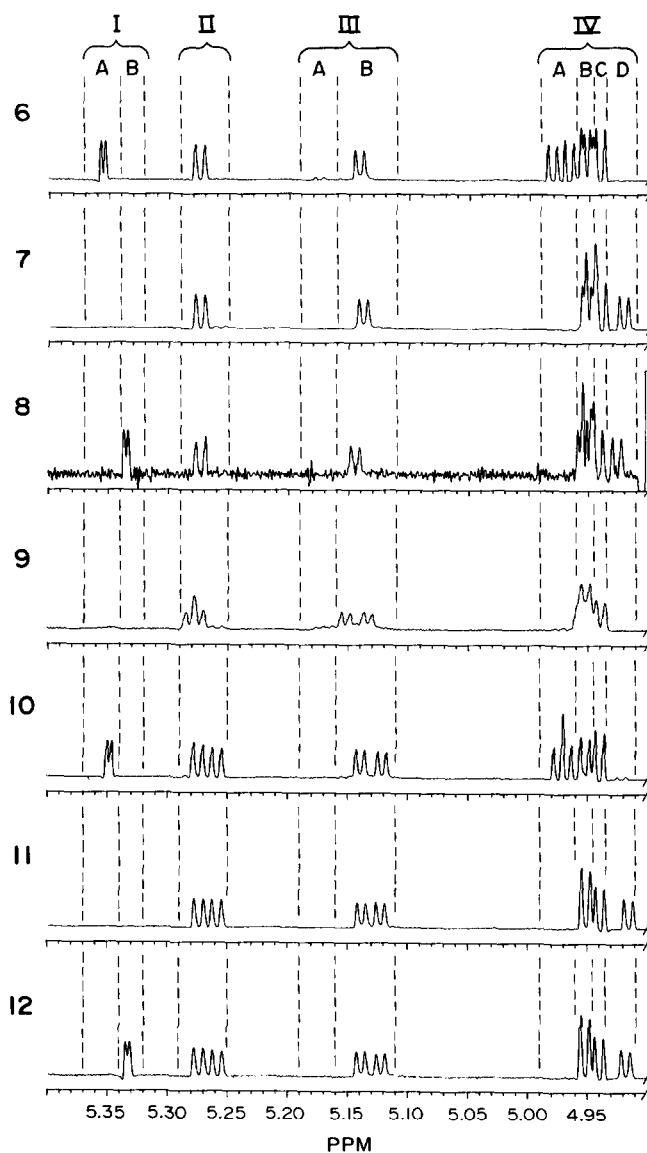


Fig. 4. Selected regions of the  $^1\text{H}$ -n.m.r. spectra of 6-12. The  $^1\text{H}$ -n.m.r. spectra were divided into nine regions, designated I-IX, corresponding to the chemical shifts of resonances that are diagnostic for different structural features of the oligoglycosyl alditols (see text for a complete description). Region V is obscured in one-dimensional spectra by the HDO resonance and associated sidebands and is not shown. The arrows in region VIII indicate the broad signals assigned to H-6 of a  $\beta$ -Glc residue. Fig. 4 continued overleaf.

**$^1\text{H}$ -N.m.r. spectral analyses of XG OAs.** — We have previously reported<sup>5,7</sup> correlations between the structural features of primary XG OAs with resonances in seven, well-defined regions of their  $^1\text{H}$ -n.m.r. spectra. These correlations are useful in deducing many of the structural features of the seven OAs whose structures are described herein (Fig. 4).

Nine regions of the  $^1\text{H}$ -n.m.r. spectrum, designated I through IX (Table I, Fig. 4), are defined in this paper. This reflects additional complexity of the spectra compared to previous reports<sup>5,7</sup>. Each region, encompassing resonances of one or more specific types of glycosyl residues, is divided into subregions that correlate with various electronic

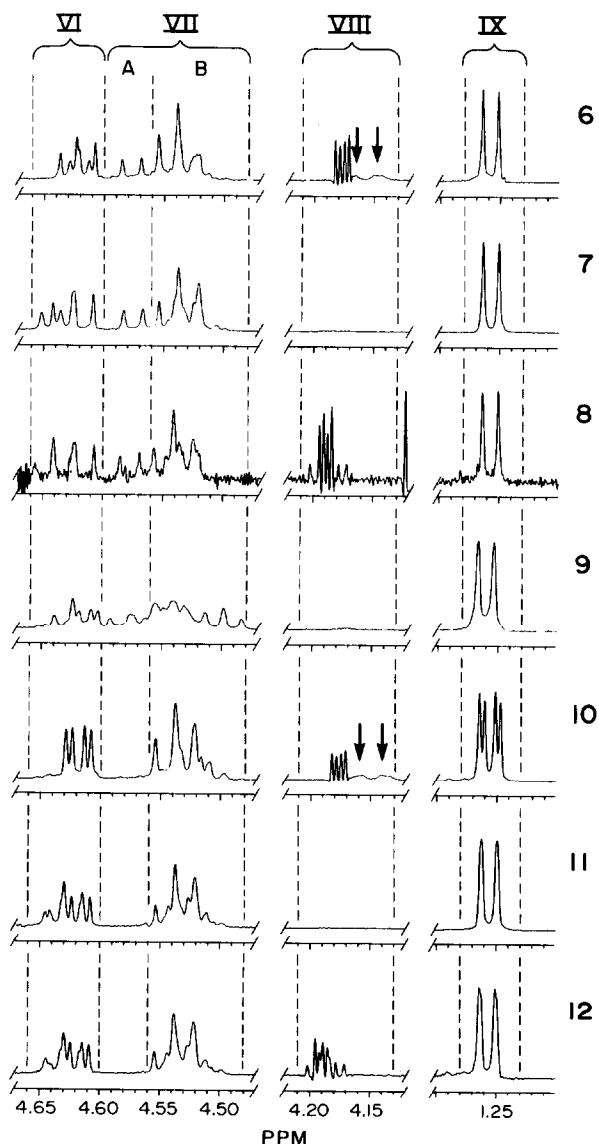


Fig. 4 continued.

TABLE I

Subregions in the  $^1\text{H}$ -n.m.r. spectra of XG oligoglycosyl alditols

Subregion	Range (ppm) <sup>a</sup>	Included resonances
I-A	5.340–5.370	H-1 of terminal $\alpha$ -Ara linked to $\beta$ -Glc C-2
I-B	5.320–5.340	H-1 of terminal $\alpha$ -Ara linked to $\beta$ -Xyl C-3
II	5.250–5.290	H-1 of terminal $\alpha$ -Fuc
III-A	5.155–5.190	H-1 of 2-linked $\alpha$ -Xyl with terminal $\beta$ -Gal at C-2
III-B	5.110–5.155	H-1 of 2-linked $\alpha$ -Xyl with 2-linked $\beta$ -Gal at C-2
IV-A	4.960–4.990	H-1 of terminal $\alpha$ -Xyl <sup>b</sup> and $\alpha$ -Xyl <sup>c</sup> when an $\alpha$ -Ara is present on C-2 of $\beta$ -Glc <sup>c</sup>
IV-B	4.945–4.960	H-1 of terminal $\alpha$ -Xyl at C-6 of 4,6-linked $\beta$ -Glc (with no chemical shift effects due to $\alpha$ -Ara or $\beta$ -Xyl residues)
IV-C	4.935–4.945	H-1 of terminal $\alpha$ -Xyl residues at C-6 of <i>unbranched</i> 6-linked $\beta$ -Glc
IV-D	4.910–4.935	H-1 of terminal $\alpha$ -Xyl <sup>b</sup> when a $\beta$ -Xyl is present on C-2 of $\beta$ -Glc <sup>c</sup>
V-A	4.750–4.790	H-1 of 3-linked $\beta$ -Xyl
V-B	4.710–4.750	H-1 of terminal $\beta$ -Xyl
VI	4.600–4.660	H-1 of 4,6-linked $\beta$ -Glc attached to C-4 of GlcOl H-1 of 2,4,6-linked $\beta$ -Glc H-1 of 2-linked $\beta$ -Gal
VII-A	4.560–4.600	H-1 of 4,6-linked $\beta$ -Glc <sup>b</sup> when no $\alpha$ -Fuc-(1 $\rightarrow$ 2)-b-Gal-(1 $\rightarrow$ 2)-moiety is present on Xyl <sup>a</sup>
VII-B	4.480–4.560	H-1 of 6-linked and 4,6-linked $\beta$ -Glc not assigned in subregions VI or VII-A H-1 of terminal $\beta$ -Gal H-5 of terminal $\alpha$ -Fuc
VIII	4.130–4.210	H-2 of terminal $\alpha$ -Ara H-4 of terminal $\alpha$ -Ara linked to $\beta$ -Xyl C-3
IX	1.230–1.280	H-6 of terminal $\alpha$ -Fuc

<sup>a</sup>The chemical shift range of the center of the multiplet is indicated and does not necessarily include all of the lines in the multiplet.

environments of the residue and thus with specific substructures. Structures were proposed for compounds **6–12** based on analysis of their one- and two-dimensional  $^1\text{H}$ -n.m.r. spectra (Table II). Certain features of these structures, such as the glycosyl sequence, glycosyl linkage, and relative position of sidechains, could not be unambiguously deduced by the  $^1\text{H}$ -n.m.r. techniques that were used. These features were firmly established by analysis of glycosyl-residue (Table III) and glycosyl-linkage (Table IV) composition and by f.a.b.-m.s. The combined chemical and spectroscopic data was then reevaluated to establish the correlations between OA structure and the presence of resonances in the nine spectral regions defined here. These correlations are described in the following paragraphs.

Region I encompasses the H-1 resonances of terminal  $\alpha$ -Araf residues (Fig. 4). The  $^1\text{H}$ -n.m.r. spectra of OAs **6**, **8**, **10**, and **12** each include one resonance in region I, indicating that these OAs each contain a single terminal  $\alpha$ -Araf residue. The presence of a 3-linked  $\beta$ -Xylp residue of **12** correlates with a slight upfield shift of the H-1 resonance of the terminal  $\alpha$ -Araf resonance (Fig. 4, Table II), providing a rationale for dividing region I into subregions I-A and I-B (see below). The H-1 resonances of  $\alpha$ -Araf residues



Residue <sup>b</sup>	Proton	<i>Oligoglycosyl alditol</i>						
		6	7	8	9	10	11	12
Xyl <sup>c</sup>	H-1	4.940	4.940	4.941	4.939	4.939	4.939	4.939
	<i>J</i> <sub>1,2</sub>	(3.6)	(3.8)	(3.7)	(3.5)	(3.6)	(3.6)	(3.6)
	H-2	3.55	3.54	n.a.	n.a.	3.54	3.54	3.54
	<i>J</i> <sub>2,3</sub>	n.a.	(10)	n.a.	n.a.	n.a.	n.a.	(10)
Gal <sup>a</sup>	H-1	— <sup>f</sup>	—	—	—	4.621	4.622	4.621
	<i>J</i> <sub>1,2</sub>	—	—	—	—	(7.7)	(7.7)	(7.8)
	H-2	—	—	—	—	3.72	3.71	3.71
	<i>J</i> <sub>2,3</sub>	—	—	—	—	(10)	(10)	(10)
Gal <sup>a'</sup>	H-1	4.615	4.616	4.615	4.616	4.615	4.615	4.616
	<i>J</i> <sub>1,2</sub>	(7.7)	(7.7)	(8.0)	(7.5)	(7.8)	(7.7)	(7.7)
	H-2	3.72	3.72	n.a.	n.a.	3.72	3.72	3.72
	<i>J</i> <sub>2,3</sub>	(9)	(10)	n.a.	n.a.	(10)	(10)	(10)
Gal <sup>b'</sup>	H-1	—	—	—	4.610	—	—	—
	<i>J</i> <sub>1,2</sub>	—	—	—	(7.8)	—	—	—
Fuc <sup>a</sup>	H-1	—	—	—	—	5.258	5.258	5.258
	<i>J</i> <sub>1,2</sub>	—	—	—	—	(4.0)	(3.8)	(4.0)
	H-2	—	—	—	—	3.79	3.79	3.79
	<i>J</i> <sub>2,3</sub>	—	—	—	—	(10)	(10)	(10)
	H-5	—	—	—	—	4.53	4.53	4.52
	<i>J</i> <sub>5,6</sub>	—	—	—	—	(6.7)	(6.6)	(6.6)
	H-6	—	—	—	—	1.253	1.255	1.255
Fuc <sup>a'</sup>	H-1	5.274	5.273	5.273	5.274	5.274	5.273	5.274
	<i>J</i> <sub>1,2</sub>	(3.8)	(3.8)	(4.0)	(3.6)	(4.0)	(4.0)	(4.0)
	H-2	3.80	3.80	n.a.	n.a.	3.80	3.80	3.80
	<i>J</i> <sub>2,3</sub>	(10)	(10)	n.a.	n.a.	(10)	(10)	(10)
	H-5	4.54	4.53	n.a.	n.a.	4.53	4.53	4.52
	<i>J</i> <sub>5,6</sub>	(6.6)	(6.6)	(6.6)	(6.8)	(6.6)	(6.6)	(6.7)
	H-6	1.258	1.257	1.257	1.260	1.258	1.257	1.257
Fuc <sup>b'</sup>	H-1	—	—	—	5.281	—	—	—
	<i>J</i> <sub>1,2</sub>	—	—	—	(3.6)	—	—	—
	<i>J</i> <sub>5,6</sub>	—	—	—	(6.8)	—	—	—
	H-6	—	—	—	1.260	—	—	—
β-Xyl	H-1	—	4.729	n.a.	—	—	4.727	4.77
	<i>J</i> <sub>1,2</sub>	—	(7.8)	(8.0)	—	—	(7.9)	(7.7)
	H-2	—	3.315	3.475	—	—	3.313	3.471
	<i>J</i> <sub>2,3</sub>	—	(9.3)	(9.1)	—	—	(9.3)	(9.2)
	H-3	—	3.450	n.a.	—	—	3.449	3.61
	<i>J</i> <sub>3,4</sub>	—	(9.0)	n.a.	—	—	(9.3)	(9)
	H-4	—	3.61	n.a.	—	—	3.61	3.68
	<i>J</i> <sub>4,5a</sub>	—	(10.6)	(10.7)	—	—	(10.6)	(10)
	<i>J</i> <sub>4,5c</sub>	—	(5.1)	n.a.	—	—	(6)	(5)
	H-5 <sub>a</sub>	—	3.263	3.296	—	—	3.263	3.298
	<i>J</i> <sub>5a,5c</sub>	—	(-11.4)	(-11.7)	—	—	(-11.3)	(-11)
	H-5 <sub>c</sub>	—	3.93	n.a.	—	—	3.93	3.96

(continued)

TABLE II (continued)

Residue <sup>b</sup>	Proton	Oligoglycosyl alditol						
		6	7	8	9	10	11	12
Ara	H-1	5.354	—	5.335	—	5.348	—	5.332
	<i>J</i> <sub>1,2</sub>	(1.8)	—	(1.8)	—	(1.8)	—	(1.8)
	H-2	4.176	—	4.189	—	4.176	—	4.190
	<i>J</i> <sub>2,3</sub>	(3.8)	—	(3.5)	—	(3.6)	—	(3.3)
	H-3	3.94	—	n.a.	—	3.94	—	3.97
	<i>J</i> <sub>3,4</sub>	(6)	—	n.a.	—	(6)	—	(6)
	H-4	4.058	—	4.185	—	4.056	—	4.186
	<i>J</i> <sub>4,5</sub>	(6)	—	n.a.	—	(6)	—	(6)
	<i>J</i> <sub>4,5'</sub>	(3)	—	n.a.	—	(3)	—	(3)
	H-5	3.69	—	n.a.	—	3.69	—	3.71
	<i>J</i> <sub>5,5'</sub>	(-11)	—	n.a.	—	(-12)	—	(-12)
	H-5'	3.83	—	n.a.	—	3.81	—	3.82

<sup>a</sup>Chemical shifts are in p.p.m. and coupling constants are in Hz. <sup>b</sup>Superscripts a, b, c, a', b', c', and s indicate the position of the residue *vis à vis* the Glcol residue. <sup>c</sup>The designation n. a. indicates that the parameter was not assigned. <sup>d</sup>The proton could not be assigned to a specific resonance, but could be assigned to one of several resonances in the spectral subregion indicated (see Table I). <sup>e</sup>The assignments of H-1 resonances of Xyl<sup>b</sup> and Xyl<sup>c</sup> may have to be reversed (see text). <sup>f</sup>Dashes indicate that no such resonance exists.

TABLE III

Glycosyl-composition of oligoglycosyl alditols 6–12<sup>a</sup>

Residue	Oligoglycosyl alditol						
	6	7	8	9	10	11	12
Fuc	0.9	1.0	1.1	1.8	2.0	1.9	2.2
Ara	0.8	0.0	0.9	0.0	0.8	0.0	1.0
Xyl	5.5	6.6	6.5	5.6	5.7	6.5	6.7
Gal	1.0	1.0	1.0	2.0	2.0	2.0	2.0
Glc	7.6 <sup>b</sup>	7.7 <sup>b</sup>	7.5 <sup>b</sup>	7.7 <sup>b</sup>	7.5 <sup>b</sup>	7.7 <sup>b</sup>	7.8 <sup>b</sup>

<sup>a</sup>Molar ratios relative to Gal (1 or 2 per molecule). <sup>b</sup>Includes the Glcol residue.

attached to C-2 of 2,4,6-linked  $\beta$ -Glc<sub>p</sub> residues (as in 6 and 10) are found in subregion I-A; H-1 resonances of  $\alpha$ -Araf residues attached to C-3 of 3-linked  $\beta$ -Xyl<sub>p</sub> residues (as in 8 and 12) are found in subregion I-B. Several other correlations involving  $\alpha$ -Araf residues and <sup>1</sup>H-n.m.r. resonances were deduced and are discussed below.

Region II resonances correspond to H-1 protons of terminal  $\alpha$ -Fuc<sub>p</sub> residues. Examination of region II in the <sup>1</sup>H-n.m.r. spectra of the seven OAs indicated that a single terminal  $\alpha$ -Fuc<sub>p</sub> residue is present in 6–8 and that two terminal  $\alpha$ -Fuc<sub>p</sub> residues are present in 9–12. The signal pattern in region II of the spectrum of 9 is somewhat different from that in the spectra of 10–12, suggesting that at least one of the  $\alpha$ -Fuc<sub>p</sub> residues in 9 is in an unusual environment (see below).

Region III resonances correspond to 2-linked  $\alpha$ -Xyl<sub>p</sub> residues, encompassing the H-1 resonances of  $\alpha$ -Xyl<sub>p</sub> residues that are substituted at C-2 with either a  $\beta$ -D-Galp

TABLE IV

Glycosyl-linkage compositions of oligoglycosyl alditols 6–12<sup>a</sup>

Residue	Ion <sup>b</sup> m/z	Oligoglycosyl alditol						
		6 <sup>c</sup>	7	8	9	10	11	12
4-Glcol <sup>d</sup>	249	0.5	0.7	0.9	1.0	0.6	0.9	0.6
T-Arap	118	1.0	0.1	1.3	0.1	1.1	0.1	1.0
T-Fucp	118	1.0	1.2	1.2	1.8	1.8	1.8	1.9
T-Xylp	118	5.0	7.1	5.3	4.5	4.5	5.2	5.6
3-Xylp	118	0.2 <sup>e</sup>	0.2 <sup>e</sup>	1.3	0.1 <sup>e</sup>	0.3	0.2 <sup>e</sup>	1.0
2-Xylp	190	1.0	1.1	1.0	1.5	1.5	1.6	1.7
2-Galp	190	1.0	1.2	1.3	2.0	1.6	2.0	1.9
6-Glcp	118	1.0 <sup>f</sup>	1.0 <sup>f</sup>	1.0 <sup>f</sup>	1.0 <sup>f</sup>	1.0 <sup>f</sup>	1.0 <sup>f</sup>	1.0 <sup>f</sup>
4-Glcp	118	1.0	1.0	1.1	1.0	1.1	1.1	1.1
4,6-Glcp	118	4.0	4.6	3.8	4.3	4.2	4.5	5.2
3,4,6-Glcp <sup>g</sup>	118	0.1 <sup>e</sup>	0.1 <sup>e</sup>	0.1 <sup>e</sup>	0.2 <sup>e</sup>	0.1 <sup>e</sup>	0.1 <sup>e</sup>	0.1 <sup>e</sup>
2,4,6-Glcp	190	1.0	1.1	0.9	0.2 <sup>e</sup>	1.2	1.2	1.3

<sup>a</sup>Molar ratios. <sup>b</sup>Residues quantitated by integration of selected-ion chromatogram obtained by g.l.c.–m.s. (see text). <sup>c</sup>Compound 6 was used as a standard for quantitation of PMAAs. <sup>d</sup>Recoveries of the derivative of 4-Glcol were extremely variable due to its volatility. Therefore, quantitation of 4-Glcol was not accurate. <sup>e</sup>Recovery of 0.3 equiv. or less indicates that the PMAA derivative is most likely an artifact of under-methylation. <sup>f</sup>Molar ratios are normalized by setting the recovery of the PMAA derivative of 6-Glc to 1. <sup>g</sup>The PMAA derivative of 3,4,6-linked Glcp is included to indicate the extent of under-methylation and does not indicate that this residue is present in any of these oligoglycosyl alditols.

moiety (subregion III-A) or an  $\alpha$ -L-Fucp-(1→2)- $\beta$ -D-Galp moiety (subregion III-B). (See ref. 5 for examples of OAs with resonances in subregion III-A.) Examination of subregion III-B confirmed the conclusions obtained by examining region II. That is, the <sup>1</sup>H-n.m.r. spectra of 6–8 each include one resonance in subregion II and one resonance in subregion III-B; the <sup>1</sup>H-n.m.r. spectra of 9–12 each include two resonances in subregion II and two resonances in subregion III-B. Thus, 6–8 each have a single  $\alpha$ -L-Fucp- $\beta$ -D-Galp- $\alpha$ -D-Xylp sidechain, while 9–12 each have two such sidechains. No resonances were observed in subregion III-A of the <sup>1</sup>H-n.m.r. spectra of the seven OAs described in this manuscript, as none contain a  $\beta$ -D-Galp- $\alpha$ -D-Xylp sidechain.

Region IV resonances correspond to H-1 of terminal  $\alpha$ -Xylp residues and are diagnostic of the branching patterns of the OAs. The chemical shifts of these resonances depend on (i) the position of the terminal  $\alpha$ -Xylp residues on the backbone and (ii) the identity and relative position of other (i.e.,  $\alpha$ -Araf and/or  $\beta$ -Xylp) glycosyl residues attached to the backbone. The presence of  $\alpha$ -Araf and  $\beta$ -Xylp residues also correlates with resonances in regions I, V, VIII, and IX (see below).

The positions of the terminal  $\alpha$ -Xyl residues in XG OAs were correlated in our previous study<sup>5</sup> to subtle differences in chemical shift of their anomeric resonances, allowing H-1 resonances of terminal  $\alpha$ -Xylp residues attached to 6-linked  $\beta$ -Glcp residues (subregion IV-C) to be differentiated from H-1 resonances of terminal  $\alpha$ -Xylp residues that are attached to 4,6-linked  $\beta$ -Glcp residues (subregion IV-B). However, correlating region IV resonances with XG structural features is made more complicated

by the presence of  $\alpha$ -Araf and  $\beta$ -Xylp residues. Two doublets are present in subregion IV-A of the  $^1\text{H}$ -n.m.r. spectra of **6** and **10**, both of which contained a terminal  $\alpha$ -Araf residue and no  $\beta$ -Xylp residues (see regions I and V). The  $\alpha$ -Araf residue in **6** was previously shown<sup>7</sup> to be attached to C-2 of a 2,4,6-linked  $\beta$ -Glc p residue in the main chain. The combined chemical and spectroscopic data indicates that this structural feature is also present in **10**, and, therefore, the doublets in subregion IV-A were assigned as H-1 resonances of  $\alpha$ -Xylp residues that were shifted downfield by the presence of an  $\alpha$ -Araf residue at C-2 of a 2,4,6-linked  $\beta$ -Glc p residue in the backbone. Based on conformational energy calculations (GEGOP)<sup>10</sup> for small XG oligosaccharides (data not shown), it was concluded that a substituent at C-2 of Glc<sup>c</sup> would interact more strongly with  $\alpha$ -Xyl<sup>b</sup> than with  $\alpha$ -Xyl<sup>c</sup>, and, therefore, resonances of  $\alpha$ -Xyl<sup>b</sup> are more likely to be affected than those of  $\alpha$ -Xyl<sup>c</sup> by the substituent at C-2 of Glc<sup>c</sup>. Therefore, the more deshielded (downfield) H-1 resonance in subregion IV-A was tentatively assigned as  $\alpha$ -Xyl<sup>b</sup> and the less deshielded as  $\alpha$ -Xyl<sup>c</sup>.

Conversely, the observation of a slightly upfield doublet (subregion IV-D) in the spectra of **7**, **8**, **11**, and **12** correlated with the presence of a  $\beta$ -Xylp residue (see region V), indicating that the  $\beta$ -Xylp residue has a slight shielding effect on H-1 of a nearby  $\alpha$ -Xylp residue. The resonance in subregion IV-D was tentatively assigned to H-1 of  $\alpha$ -Xyl<sup>b</sup>, based on assumption that  $\alpha$ -Xyl<sup>b</sup> would be strongly affected by a substituent at C-2 of Glc<sup>c</sup> (see above). The spectrum of **9** contains no resonances in subregions IV-A or IV-D, consistent with the absence of  $\alpha$ -Araf and  $\beta$ -Xylp residues in this OA.

Region V encompasses H-1 resonances of  $\beta$ -Xylp residues. These novel resonances were first detected in the COSY spectra of **7**, **11**, and **12**. The  $^1\text{H}$ -spin systems coupled to these  $\beta$ -anomeric protons were analyzed by COSY<sup>11</sup> and/or 1-D HOHAHA<sup>12</sup> spectroscopy (Table II). Analysis of the chemical shifts and coupling signatures of these spin systems indicated that a single  $\beta$ -Xyl residue was present in each of these OAs. The characteristic downfield shift of  $^1\text{H}$ -resonances (especially H-3) of the  $\beta$ -Xylp residue of **12** relative to the corresponding resonances of **7** and **11** suggests that **12** contains a 3-linked  $\beta$ -Xylp residue and that **7** and **11** contain a terminal  $\beta$ -Xylp residue. The presence in **12** of an  $\alpha$ -Araf residue, indicated by a resonance in region I, correlates with the downfield shifts of the  $\beta$ -Xylp resonances. In addition, no signals were observed in subregion IV-A of the  $^1\text{H}$ -n.m.r. spectrum of **12**. This suggests that the  $\alpha$ -Araf residue in **12** is attached to a different site than in **6** and **10**, as attachment of  $\alpha$ -Araf residues directly to C-2 of a main chain  $\beta$ -Glc p residue would shift the H-1 resonances of two  $\alpha$ -Xylp residues into subregion IV-A. These results, in combination with the results of glycosyl-linkage and f.a.b.-m.s. analyses (see below), indicate that the  $\alpha$ -Araf residue of **12** is attached to C-3 of the  $\beta$ -Xylp residue. This conclusion is consistent with shifts in the positions of the H-4 resonances of the  $\alpha$ -Araf residues and of the H-6 resonances of  $\beta$ -Glc p residues (see below, region VIII). These chemical shift effects depend on whether the  $\alpha$ -Araf residue is attached directly to the main chain, as in **6** and **10**, or through an intervening  $\beta$ -Xylp residue, as in **12**. Region V was therefore divided into subregions V-A (H-1 of 3-linked  $\beta$ -Xylp residues) and V-B (H-1 of terminal  $\beta$ -Xylp residues).

Region VI includes the H-1 resonances of 2,4,6-linked  $\beta$ -Glc p residues, the H-1



resonances of 2-linked  $\beta$ -Galp residues, and the H-1 resonances of 4,6-linked  $\beta$ -Glc p residues that are linked directly to the alditol (*i.e.*, Glc<sup>a</sup>)<sup>5</sup>. A correlation was established between an H-1/H-2 crosspeak at  $\delta$ ,4.643,  $\delta$ ,3.60 in the COSY spectrum of **6** and the presence of a 2,4,6-linked  $\beta$ -Glc p residue. The diagnostic crosspeak was present in the COSY spectra of **7**, **10**, **11**, and **12**, indicating that each of these OAs contains a single 2,4,6-linked  $\beta$ -Glc p residue. Evaluation of regions II and III-B indicates that **6–8** each contain one 2-linked  $\beta$ -Galp residue and that **9–12** each have two 2-linked  $\beta$ -Galp residues, each of which give rise to one H-1 resonance in region VI. The anomeric proton of the  $\beta$ -Glc p residue attached to the Glc ol also gives rise to one H-1 resonance in region VI. Taking these resonances into account, integration of the signal areas in region VI indicates that **9** has no 2,4,6-linked  $\beta$ -Glc p residues and that the other six OAs each have one 2,4,6-linked glucosyl residue. This result was consistent with the results of glycosyl-linkage (Table IV) and f.a.b.-m.s. analyses (see below). We conclude that  $\alpha$ -Araf- and/or  $\beta$ -Xylp-containing sidechains are attached to C-2 of the 2,4,6-linked  $\beta$ -glucosyl residue in **6**, **7**, **8**, **10**, **11**, and **12**.

Region VII includes the H-1 resonances of those 4,6-linked  $\beta$ -Glc p residues not assigned to region VI, the H-1 resonances of 6-linked  $\beta$ -Glc p residues, and the H-5 resonances of  $\alpha$ -Fucp residues<sup>5</sup>. The resonance in subregion VII-A of the <sup>1</sup>H-n.m.r. spectra of **6–9** was assigned to H-1 of  $\beta$ -Glc<sup>b</sup> for the following reasons. (i) The anomeric proton of  $\beta$ -Glc<sup>b</sup> in **13** (the reduced form of **2**) is in an environment similar to that of H-1 of  $\beta$ -Glc<sup>b</sup> in **6–9**, and gives rise to a resonance found in subregion VII-A ( $\delta$ 4.586)<sup>5</sup>. (ii) The resonance in subregion VII-A clearly arises from H-1 of a  $\beta$ -pyranosyl residue, but is not the H-1 resonance of  $\beta$ -Glc<sup>a</sup>,  $\beta$ -Glc<sup>c</sup>, or  $\beta$ -Gal (which have been assigned to other subregions). (iii) Resonances in subregion VII-A of the <sup>1</sup>H-n.m.r. spectra of **6–9** correlate with the absence of an  $\alpha$ -Fuc-(1 $\rightarrow$ 2)- $\beta$ -Gal-(1 $\rightarrow$ 2)-Xyl sidechain at C-6 of  $\beta$ -Glc<sup>a</sup>. Changes in the structure of the sidechain attached to  $\beta$ -Glc<sup>a</sup> would most likely affect the H-1 resonances of  $\beta$ -Glc<sup>a</sup>,  $\beta$ -Glc<sup>b</sup>, and perhaps  $\beta$ -Glc<sup>c</sup>, but not those of  $\beta$ -Glc<sup>a'</sup>,  $\beta$ -Glc<sup>b'</sup> or  $\beta$ -Glc<sup>c'</sup>. Therefore, the assignment of the H-1 resonance of  $\beta$ -Glc<sup>b</sup> of **6–9** to subregion VII-A was established by the process of elimination (*i.e.*, combining *ii* and *iii*).

Region VIII encompasses H-2 resonances of terminal  $\alpha$ -Araf residues, as determined by analysis of the COSY spectra of **6**, **10**, and **12** (Table II). When the OA contains an  $\alpha$ -Araf residue but no  $\beta$ -Xylp residue (**6** and **10**), region VIII also includes a very broad resonance assigned as H-6 of one of the  $\beta$ -Glc p residues. (The physical basis of this extreme line broadening is currently under investigation.) However, the  $\beta$ -Glc p H-6 resonance was not present in region VIII when both  $\alpha$ -Araf and  $\beta$ -Xylp residues were present in the OA (**8** and **12**). In this case, the H-4 resonance of the  $\alpha$ -Araf residue was observed in region VIII. These chemical shift effects suggest that, when the  $\alpha$ -Araf residue is attached directly to the main chain (*i.e.*, no  $\beta$ -Xylp residue is present as in **6** and **10**), H-6 of a nearby  $\beta$ -Glc p residue is deshielded. Conversely, the presence of a  $\beta$ -Xylp residue shifts H-4 of the  $\alpha$ -Araf residue downfield into region VIII, suggesting that the  $\beta$ -Xylp residue is closely associated with the  $\alpha$ -Araf residue (when both are present). Glycosyl-linkage analysis and other chemical shift effects (see above) indicate that when  $\alpha$ -Araf and  $\beta$ -Xylp residues are both present (**8** and **12**), the  $\beta$ -Xylp residue is 3-linked,

but when no  $\alpha$ -Araf residue is present (7 and 11), the  $\beta$ -Xylp residue is terminal. These observations, along with the results of f.a.b.-m.s. and glycosyl-linkage composition analyses (see below) indicate that an  $\alpha$ -Araf-(1 $\rightarrow$ 3)- $\beta$ -Xylp- sidechain is attached to C-2 of a  $\beta$ -Glc p residue in 8 and 12.

Region IX includes the H-6 resonances of the terminal  $\alpha$ -Fuc residues.

The yield of 8 was relatively low, and, therefore, 8 was not analyzed by two-dimensional  $^1\text{H}$ -n.m.r. spectroscopy. However, a significant portion of the structure of 8 can be deduced by applying the correlations described above to the one-dimensional  $^1\text{H}$ -n.m.r. spectrum of 8 (Fig. 4). For example, the resonances in region VIII and subregions I-B and IV-D of the  $^1\text{H}$ -n.m.r. spectrum of 8 indicate the presence of an  $\alpha$ -Araf-(1 $\rightarrow$ 2)- $\beta$ -Xylp sidechain at C-2 of a 2,4,6-linked  $\beta$ -Glc p residue. The resonances in regions II and III-B indicate that 8 has a single  $\alpha$ -Fuc-(1 $\rightarrow$ 2)- $\beta$ -Gal-(1 $\rightarrow$ 2)-Xyl sidechain. This interpretation is consistent with the results of glycosyl-residue composition (Table III), glycosyl-linkage composition analysis (Table IV), and analysis by f.a.b.-m.s. (see below).

*Glycosyl-linkage analysis.* — The glycosyl residues of the seven OAs were converted to their partially methylated alditol acetate (PMAA) derivatives for analysis of their glycosyl-linkage compositions<sup>13,14</sup>. Inaccurate quantitation of the glycosyl-linkage composition of a sample often results when differences in the chemical stability of glycosyl residues or their derivatives lead to significant differences in the relative recoveries of the various PMAAs<sup>15</sup>. We used a highly purified preparation of the previously characterized 6 as a standard compound for glycosyl-linkage analysis in order to account for the differential reactivity of the glycosyl residues and thus improve the reliability of the glycosyl-linkage composition analysis (see Experimental). The glycosyl-linkage compositions of 6–12 (Table IV) that were obtained by this procedure were in good agreement with the results of the spectroscopic and other chemical analyses.

*Fast-atom bombardment-mass spectrometry.* — F.a.b.-mass spectra of per-*O*-acetylated OAs 6–12 were recorded in the positive-ion mode using thioglycerol as the matrix (Table V, Fig. 5). The f.a.b.-mass spectra of underivatized OAs 6, 7, and 9–12 were recorded in the negative-ion mode using 1-amino-2,3-dihydroxypropane as the matrix (Table VI, Fig. 6). Abundant pseudomolecular ions were observed during both types of analysis, which, in conjunction with glycosyl residue analysis (Table III), allowed the number of Ara, Fuc, Xyl, Gal, Glc, and Glc p residues in each OA to be accurately determined.

Fragment ions were observed in both types of f.a.b.-mass spectra. Fragmentation during negative-ion f.a.b.-m.s. of underivatized OAs is dominated by cleavage between C-1 and O-1 of glycosidic residues, resulting in the formation of negatively charged alditol end fragments<sup>5</sup>. Conversely, the negative-ion f.a.b.-mass spectra of reducing oligosaccharides include several different types of fragment ions, and, therefore, are not as easily interpreted as the spectra of oligoglycosyl alditols. Thus, the reductive conversion of oligosaccharides to OAs not only made purification easier (see above) but facilitated f.a.b.-m.s. analysis. The dominant fragment ions observed during positive-ion f.a.b.-m.s. of the per-*O*-acetylated OAs are also formed by cleavage of the bond

TABLE V

Positive-ion mode f.a.b.-m.s. of per-*O*-acetylated oligoglycosyl alditols 6–12

<i>Ion</i> <sup>a</sup>	<i>Nominal mass</i>	<i>Type</i> <sup>b</sup>	<i>Ion composition</i>	<i>Parent oligoglycosyl alditol</i>							
<b>A</b>	273	[A] <sup>+</sup>	Fuc	6	7	8	9	10	11	12	
<b>B</b>	561	[A] <sup>+</sup>	FucGal	6	7	8	9	10	11	12	
<b>C</b>	777	[A] <sup>+</sup>	FucGalXyl	6	7	8	9	10	11	12	
<b>D</b>	259	[A] <sup>+</sup>	Xyl	6	7	8	9	10	11	12	
<b>D'</b>	259	[A] <sup>+</sup>	Ara	6		8		10		12	
<b>E</b>	547	[A] <sup>+</sup>	XylGlc	6	7	8	9	10	11	12	
<b>F</b>	1051	[A] <sup>+</sup>	Xyl <sub>2</sub> Glc <sub>2</sub>	6	7	8	c	10	11	12	
<b>G</b>	2361	[A] <sup>+</sup>	FucGalXyl <sub>3</sub> Glc <sub>4</sub>	6	7	8		10	11	12	
<b>H</b>	2879	[A] <sup>+</sup>	Fuc <sub>2</sub> Gal <sub>2</sub> Xyl <sub>3</sub> Glc <sub>4</sub>				9				
<b>I</b>	3081	[A] <sup>+</sup>	AraFucGalXyl <sub>4</sub> Glc <sub>5</sub>	6				10			
<b>P</b>	3081	[A] <sup>+</sup>	FucGalXyl <sub>3</sub> Glc <sub>5</sub>		7				11		
<b>J</b>	3297	[A] <sup>+</sup>	AraFucGalXyl <sub>3</sub> Glc <sub>5</sub>			8				12	
<b>K</b>	475	[A] <sup>+</sup>	AraXyl			8				12	
	4498	[M + NH <sub>4</sub> ] <sup>+</sup>	AraFucGalXyl <sub>6</sub> Glc <sub>7</sub> Glc <sub>ol</sub>	6							
	4498	[M + NH <sub>4</sub> ] <sup>+</sup>	FucGalXyl <sub>7</sub> Glc <sub>7</sub> Glc <sub>ol</sub>		7						
	4714	[M + NH <sub>4</sub> ] <sup>+</sup>	AraFucGalXyl <sub>7</sub> Glc <sub>7</sub> Glc <sub>ol</sub>			8					
	4800	[M + NH <sub>4</sub> ] <sup>+</sup>	Fuc <sub>2</sub> Gal <sub>2</sub> Xyl <sub>6</sub> Glc <sub>7</sub> Glc <sub>ol</sub>				9				
	5016	[M + NH <sub>4</sub> ] <sup>+</sup>	AraFuc <sub>2</sub> Gal <sub>2</sub> Xyl <sub>6</sub> Glc <sub>7</sub> Glc <sub>ol</sub>					10			
	5016	[M + NH <sub>4</sub> ] <sup>+</sup>	Fuc <sub>2</sub> Gal <sub>2</sub> Xyl <sub>7</sub> Glc <sub>7</sub> Glc <sub>ol</sub>						11		
	5232	[M + NH <sub>4</sub> ] <sup>+</sup>	AraFuc <sub>2</sub> Gal <sub>2</sub> Xyl <sub>7</sub> Glc <sub>7</sub> Glc <sub>ol</sub>							12	
<i>d</i>	4503	[M + Na] <sup>+</sup>	AraFucGalXyl <sub>7</sub> Glc <sub>7</sub> Glc <sub>ol</sub>	6							
<i>d</i>	4503	[M + Na] <sup>+</sup>	FucGalXyl <sub>7</sub> Glc <sub>7</sub> Glc <sub>ol</sub>		7						
<i>d</i>	4719	[M + Na] <sup>+</sup>	AraFucGalXyl <sub>7</sub> Glc <sub>7</sub> Glc <sub>ol</sub>			8					
<i>d</i>	4805	[M + Na] <sup>+</sup>	Fuc <sub>2</sub> Gal <sub>2</sub> Xyl <sub>6</sub> Glc <sub>7</sub> Glc <sub>ol</sub>				9				
<i>d</i>	5021	[M + Na] <sup>+</sup>	AraFuc <sub>2</sub> Gal <sub>2</sub> Xyl <sub>6</sub> Glc <sub>7</sub> Glc <sub>ol</sub>					10			
<i>d</i>	5021	[M + Na] <sup>+</sup>	Fuc <sub>2</sub> Gal <sub>2</sub> Xyl <sub>7</sub> Glc <sub>7</sub> Glc <sub>ol</sub>						11		
<i>d</i>	5237	[M + Na] <sup>+</sup>	AraFuc <sub>2</sub> Gal <sub>2</sub> Xyl <sub>7</sub> Glc <sub>7</sub> Glc <sub>ol</sub>							12	

<sup>a</sup>See Fig. 5. <sup>b</sup>See reference 16. <sup>c</sup>An ion at *m/z* 1051 in the positive-mode f.a.b.-mass spectrum of **9** was assigned as a double-cleavage ion. <sup>d</sup>Observed when NaOAc was added to f.a.b. probe tip<sup>16</sup>.

between C-1 and O-1 of glycosidic residues, but result in positively charged non-reducing-end fragments<sup>16</sup>. The two different types of f.a.b.-mass spectra thus provided complementary structural information, which allowed complete glycosyl sequences to be deduced for OAs 6–12.

Positive-ion f.a.b.-m.s. of per-*O*-acetylated OAs provided the sequences and positions of most of the sidechains (Fig. 5, Table V). For example, the fragment ions **A** at *m/z* 273 ([Fuc]<sup>+</sup>), **B** at *m/z* 561 ([FucGal]<sup>+</sup>), and **C** at *m/z* 777 ([FucGalXyl]<sup>+</sup>) confirmed that α-Fucp-(1→2)-β-Galp(1→2)-α-Xylp sidechains are present in all seven OAs. The fragment ions **D** at *m/z* 259 ([Xyl]<sup>+</sup>), **E** at *m/z* 547 ([XylGlc]<sup>+</sup>), and **F** at *m/z* 1051 ([Xyl<sub>2</sub>Glc<sub>2</sub>]<sup>+</sup>) indicated that isoprimeverose (*i.e.*, α-D-Xylp-(1→6)-D-Glcp) moieties are present at the non-reducing ends of each of the OAs. The abundant ion **K** at *m/z* 475 ([AraXyl]<sup>+</sup>) in the spectra of per-*O*-acetylated **8** and **12** confirmed that an α-Araf-(1→3)-β-Xylp sidechain was present in these two OAs.

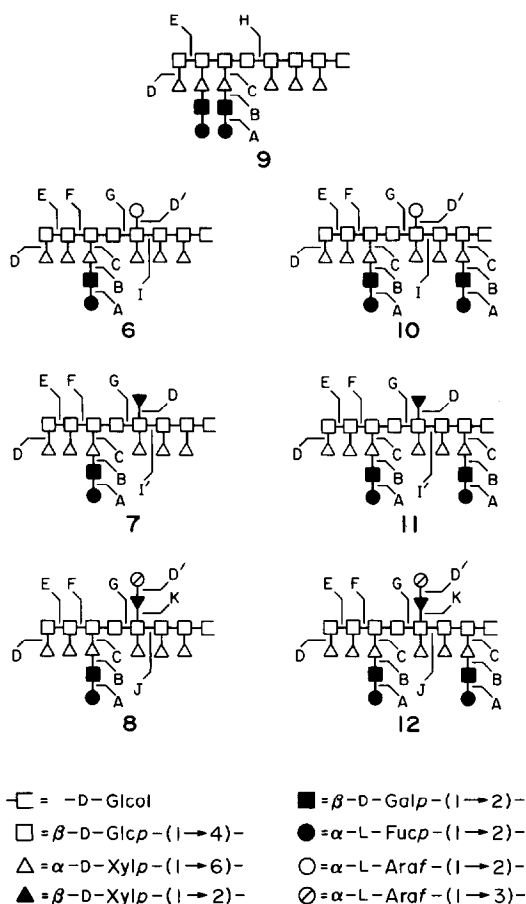


Fig. 5. Diagnostic fragmentations of per-*O*-acetylated 6–12 obtained during positive-ion f.a.b.-m.s. Fragment ions<sup>5,16</sup> were formed by cleavage of the C-1/O-1 bond, leaving a positive charge on the non-reducing end fragment. The mass of each ion is given in Table V.

Fragment ions expected at  $m/z$  1569 ( $[\text{FucGalXyl}_2\text{Glc}_2]^+$ ) and 2591 ( $[\text{Fuc}_2\text{Gal}_2\text{Xyl}_3\text{Glc}_3]^+$ ) were not observed in the spectrum of per-*O*-acetylated 9. Similarly, no fragment ion was observed at  $m/z$  2073 ( $[\text{FucGalXyl}_3\text{Glc}_3]^+$ ) in the spectra of the six other per-*O*-acetylated OAs. These “missing”  $A^+$  ions correspond to cleavage between C-1 and O-1 of  $\beta$ -Glc residues bearing  $\alpha$ -Fuc-(1 $\rightarrow$ 2)- $\beta$ -Gal-(1 $\rightarrow$ 2)-Xyl sidechains at C-6. The absence of these ions has been reported earlier<sup>17</sup> and suggests either that ion formation *via* fragmentation of the main chain  $\beta$ -Glc residue bearing an extended sidechain is inhibited or that these fragment ions readily decompose. Nevertheless, ions formed by cleavage of the main chain provide important information regarding the glycosyl sequence of the OAs. In fact, the most striking feature of the positive-ion f.a.b.-mass spectra of the per-*O*-acetylated OAs is the unusually high

TABLE VI

Negative mode f.a.b.-m.s. of underivatized oligoglycosyl alditols **6**, **7**, and **9–12**

<i>Ion<sup>a</sup></i>	<i>Nominal mass</i>	<i>Type<sup>b</sup></i>	<i>Ion composition</i>	<i>Parent oligoglycosyl alditol</i>		
<b>Z</b>	475	[B] <sup>-</sup>	XylGlcGlc	<b>6</b>	<b>7</b>	<b>9</b>
<b>Y</b>	769	[B] <sup>-</sup>	Xyl <sub>2</sub> Glc <sub>2</sub> Glc	<b>6</b>	<b>7</b>	<b>9</b>
<b>X</b>	1063	[B] <sup>-</sup>	Xyl <sub>3</sub> Glc <sub>3</sub> Glc			<b>9</b>
<b>W</b>	1225	[B] <sup>-</sup>	Xyl <sub>3</sub> Glc <sub>4</sub> Glc			<b>9</b>
<b>V</b>	1195	[B] <sup>-</sup>	AraXyl <sub>3</sub> Glc <sub>3</sub> Glc	<b>6</b>		
<b>V'</b>	1195	[B] <sup>-</sup>	Xyl <sub>4</sub> Glc <sub>3</sub> Glc		<b>7</b>	
<b>U</b>	1357	[B] <sup>-</sup>	AraXyl <sub>3</sub> Glc <sub>4</sub> Glc	<b>6</b>		
<b>U'</b>	1357	[B] <sup>-</sup>	Xyl <sub>4</sub> Glc <sub>4</sub> Glc		<b>7</b>	
<b>T</b>	785	[B] <sup>-</sup>	FucGalXyl <sub>2</sub> Glc <sub>2</sub> Glc			<b>10 11 12</b>
<b>S</b>	1079	[B] <sup>-</sup>	FucGalXyl <sub>2</sub> Glc <sub>2</sub> Glc			<b>10 11 12</b>
<b>R</b>	1505	[B] <sup>-</sup>	AraFucGalXyl <sub>3</sub> Glc <sub>3</sub> Glc			<b>10</b>
<b>R'</b>	1505	[B] <sup>-</sup>	FucGalXyl <sub>4</sub> Glc <sub>3</sub> Glc			<b>11</b>
<b>Q</b>	1667	[B] <sup>-</sup>	AraFucGalXyl <sub>3</sub> Glc <sub>4</sub> Glc			<b>10</b>
<b>Q'</b>	1667	[B] <sup>-</sup>	FucGalXyl <sub>4</sub> Glc <sub>4</sub> Glc			<b>11</b>
<b>P</b>	1637	[B] <sup>-</sup>	AraFucGalXyl <sub>4</sub> Glc <sub>3</sub> Glc			<b>12</b>
<b>O</b>	1799	[B] <sup>-</sup>	AraFucGalXyl <sub>4</sub> Glc <sub>4</sub> Glc			<b>12</b>
	2547	[M - H] <sup>-</sup>	AraFucGalXyl <sub>6</sub> Glc <sub>3</sub> Glc	<b>6</b>		
	2547	[M - H] <sup>-</sup>	FucGalXyl <sub>7</sub> Glc <sub>7</sub> Glc		<b>7</b>	
	2723	[M - H] <sup>-</sup>	Fuc <sub>2</sub> Gal <sub>2</sub> Xyl <sub>6</sub> Glc <sub>7</sub> Glc			<b>9</b>
	2855	[M - H] <sup>-</sup>	AraFuc <sub>2</sub> Gal <sub>2</sub> Xyl <sub>6</sub> Glc <sub>7</sub> Glc			<b>10</b>
	2855	[M - H] <sup>-</sup>	Fuc <sub>2</sub> Gal <sub>2</sub> Xyl <sub>6</sub> Glc <sub>7</sub> Glc			<b>11</b>
	2987	[M - H] <sup>-</sup>	AraFuc <sub>2</sub> Gal <sub>2</sub> Xyl <sub>7</sub> Glc <sub>7</sub> Glc			<b>12</b>

<sup>a</sup>See Fig. 6. <sup>b</sup>See reference 16.

abundance of fragment ions formed by cleavage of the glycosidic bond of unbranched  $\beta$ -Glc residues that are *adjacent* to  $\beta$ -Glc residues bearing  $\alpha$ -Fuc-(1 $\rightarrow$ 2)- $\beta$ -Gal-(1 $\rightarrow$ 2)-Xyl sidechains at C-6. These abundant ions were observed at  $m/z$  2879 (ion **H**, [Fuc<sub>2</sub>Gal<sub>2</sub>Xyl<sub>3</sub>Glc<sub>4</sub>]<sup>+</sup>) in the spectrum of per-*O*-acetylated **9** and at  $m/z$  2361 (ion **G**, [FucGalXyl<sub>3</sub>Glc<sub>4</sub>]<sup>+</sup>) in the spectra of the six other per-*O*-acetylated OAs. These abundant fragment ions indicate that **9** contains XG subunit **5** and the other six OAs contain XG subunit **3** at their non-reducing ends. This conclusion is consistent with chemical and <sup>1</sup>H-n.m.r. analyses and was unambiguously confirmed for **6** and **9** by analysis of fragments obtained by enzymatic cleavage of these OAs. (See the following and ref. 7 for details.)

Low-abundance ions **I**, **I'**, and **J** (Fig. 5, Table V) indicate that the unbranched Glc<sup>s</sup> residue is directly linked to the 2,4,6-linked  $\beta$ -Glc residue (bearing an  $\alpha$ -Araf,  $\beta$ -Xylp, or  $\alpha$ -Araf-(1 $\rightarrow$ 3)- $\beta$ -Xylp sidechain at C-2), except in **9**, which has no 2,4,6-linked  $\beta$ -Glc residue. This conclusion was confirmed by negative-ion f.a.b.-m.s. of the native OAs, as described next.

The sequences of glycosyl residues at the alditol end of the OAs were most readily determined by negative-ion f.a.b.-m.s. (Fig. 6, Table VI). The negative-ion f.a.b.-mass spectra of **6**, **7**, and **9** included fragment ions **Z** at  $m/z$  475 ([XylGlcGlc]<sup>-</sup>) and **Y** at  $m/z$

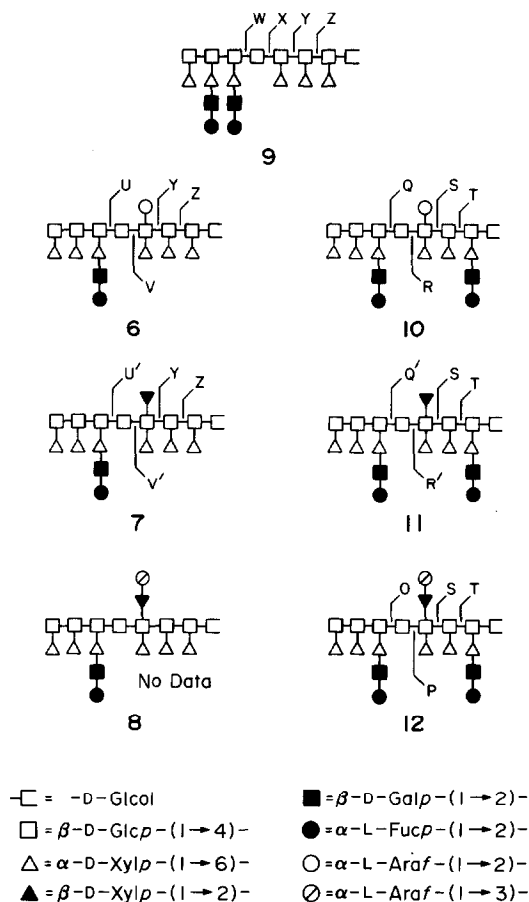


Fig. 6. Diagnostic fragmentations of underivatized **6**, **7**, and **9–12** obtained during negative-ion f.a.b.-m.s. Fragment ions<sup>5,16</sup> were formed by cleavage of the C-1/O-1 bond, leaving a negative charge on the alditol end fragment. The mass of each ion is given in Table VI.

769 ([Xyl<sub>2</sub>Glc<sub>2</sub>Glc]<sup>−</sup>), indicating that no fucosyl residue-containing sidechains were present near the alditol end of these OAs. The presence of ions **T** at *m/z* 785 ([FucGalXylGlcGlc]<sup>−</sup>) and **S** at *m/z* 1079 ([FucGalXyl<sub>2</sub>Glc<sub>2</sub>Glc]<sup>−</sup>) in the spectra of **10**, **11**, and **12** indicated that these OAs contain a Fuc-Gal-Xyl sidechain on Glc<sup>a</sup> (the residue that is attached to the Glcol moiety). The position of the 2,4,6-linked Glc residue bearing a terminal α-Araf, a terminal β-Xylp, or an α-Araf-(1→3)-β-Xylp moiety was indicated by ions **P**, **R**, **R'**, **V**, and **V'** (Fig. 6, Table VI). No fragment ions corresponding to the presence of a pentosyl or dipentosyl sidechain at C-2 of a 2,4,6-linked Glc residue were observed in the spectrum of **9**. Due to the limiting quantity of material, the quality of the negative-ion f.a.b.-mass spectrum of **8** was not adequate to obtain sequence information; consequently, the proposed structure of **8** is based on positive-ion f.a.b.-m.s., chemical analysis, and <sup>1</sup>H-n.m.r. spectroscopy.

**Endo-(1→4)- $\beta$ -D-glucanase treatment of OAs.** — The glycosidic linkage from the unbranched, 4-linked  $\beta$ -Glc<sub>p</sub> residue (Glc<sup>s</sup>) to  $\beta$ -Glc<sup>c</sup> is normally cleaved by *endo*-(1→4)- $\beta$ -D-glucanase. OAs **6–8** and **10–12** are all resistant to hydrolysis by *endo*-(1→4)- $\beta$ -D-glucanase, and all contain a sidechain at C-2 of Glc<sup>c</sup>. We previously reported<sup>7</sup> that removal of the  $\alpha$ -Araf sidechain at C-2 of Glc<sup>c</sup> of **6** results in a product that is susceptible to hydrolysis by the *endo*-(1→4)- $\beta$ -D-glucanase. However, there is no sidechain at C-2 of Glc<sup>c</sup> in **9**, and yet **9** is resistant to cleavage by the enzyme. Therefore, the relative susceptibility of **6–12** to cleavage by the *endo*-(1→4)- $\beta$ -D-glucanase was investigated (see Experimental). H.p.l.c. analysis of *endo*-(1→4)- $\beta$ -D-glucanase-treated OAs **6**, **7**, **8**, **10**, **11**, and **12** indicated that these OAs are completely resistant to cleavage by the enzyme at all concentrations tested. This result suggests that a sidechain at C-2 of Glc<sup>c</sup> sterically hinders formation of a complex involving the catalytic site of the enzyme and Glc<sup>s</sup>.

Treatment of **9** with *endo*-(1→4)- $\beta$ -D-glucanase at a concentration corresponding to the same enzyme:substrate ratio that was initially used to cleave the polymeric XG did not release any fragment oligosaccharides that could be detected by h.p.l.c. However, treatment of **9** with a 100-fold greater enzyme concentration released two fragments (A and B) that were separated by h.p.l.c. (Fig. 7). Fragment A was shown to be **13** (*i.e.*, the reduced form of **2**) by comparing its <sup>1</sup>H-n.m.r. spectrum to that of an authentic standard<sup>5</sup>. Fragment B was reduced with NaBH<sub>4</sub>, and the product was shown to be **14** (*i.e.*, the reduced form of **5**), by the same criterion<sup>17</sup>. These results confirm the structure of **9**, as determined by chemical and spectroscopic techniques, and indicate that the

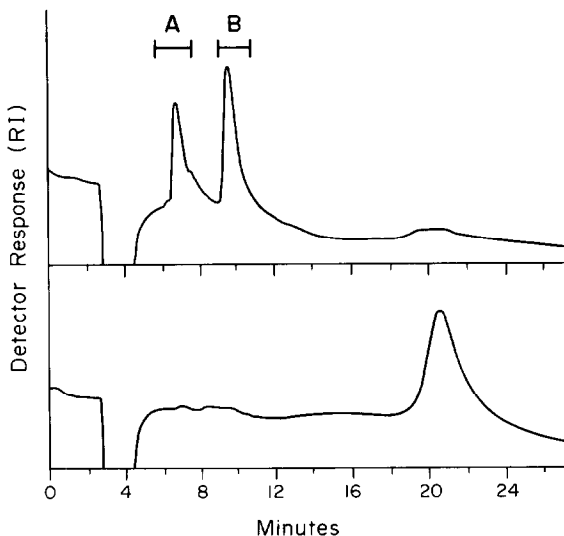


Fig. 7. H.p.l.c. analysis of products obtained upon treatment of **9** with *endo*-(1→4)- $\beta$ -D-glucanase. The digested oligoglycosyl alditol was dissolved in 100  $\mu$ L of water, applied to the Dynamax-60A h.p.l.c. column and eluted with 3:2 CH<sub>3</sub>CN:H<sub>2</sub>O. The elution profile after digestion with 0.2 U of enzyme (top) and 0.002 U of enzyme (bottom) are shown. Hydrolysis products A and B were pooled as shown.

presence of two adjacent  $\alpha$ -Fuc-(1 $\rightarrow$ 2)- $\beta$ -Gal-(1 $\rightarrow$ 2)-Xyl sidechains can render the XG OA partially resistant to cleavage by the *endo*-(1 $\rightarrow$ 4)- $\beta$ -D-glucanase. The partial susceptibility of **9** to cleavage by *endo*-(1 $\rightarrow$ 4)- $\beta$ -D-glucanase supports the concept that the structural basis for its resistance to enzymatic cleavage is different from that of **6–8** and **10–12**.

## CONCLUSIONS

A combination of  $^1\text{H}$ -n.m.r. spectroscopy, f.a.b.-mass spectrometry, and chemical analysis allowed us to determine the structures of seven oligoglycosyl alditols derived from xyloglucan. The presence of previously uncharacterized pentosyl substituents in these closely related oligoglycosyl alditols has provided a basis for determining additional correlations between the chemical shifts of certain  $^1\text{H}$ -n.m.r. resonances and specific structural features, in a manner similar to that routinely used to determine the structures of *N*-linked oligosaccharide sidechains of glycoproteins<sup>18</sup>. The correlations described here are completely consistent with those published in ref. 5. The additional correlations observed facilitate the use of one-dimensional  $^1\text{H}$ -n.m.r. spectroscopy in the structural determination of XG-derived oligoglycosyl alditols and XG polymers.

The functional significance of the unusual sidechains found at C-2 of 2,4,6-linked  $\beta$ -Glc residues is not clear. Detection of the  $\alpha$ -Araf-(1 $\rightarrow$ 3)- $\beta$ -Xylp- moiety in a plant cell wall preparation would normally indicate the presence of an arabinoxylan. The fact that this structure was covalently attached to a xyloglucan may simply indicate that some of the glycosyltransferases that assemble xylans can use xyloglucans as acceptor substrates. Alternatively, it may indicate that xyloglucans and arabinoxylans are covalently attached in the primary cell wall of *Acer pseudoplatanus*, with  $\beta$ -xylan moieties initiated at C-2 of main-chain  $\beta$ -Glc residues of the xyloglucan.

The presence of  $\alpha$ -Araf-(1 $\rightarrow$ 2)-,  $\beta$ -Xylp-(1 $\rightarrow$ 2)-, and  $\alpha$ -Araf-(1 $\rightarrow$ 3)- $\beta$ -Xylp-(1 $\rightarrow$ 2)- sidechains may have a significant effect on the rheological properties of XGs, and might modify their ability to bind to microcrystalline cellulose by destabilizing XG/cellulose interactions in localized areas of the XG polymer. This localized interruption of XG binding could result in a well-defined cellulose/XG network, where crosslinks between cellulose microfibrils correspond to XG domains that contain sidechains at C-2 of the main-chain  $\beta$ -Glc residues. The size distribution of the products obtained when sycamore extracellular XG is treated with *endo*-(1 $\rightarrow$ 4)- $\beta$ -D-glucanase (Fig. 1) provides evidence that such *endo*-(1 $\rightarrow$ 4)- $\beta$ -D-glucanase-resistant domains exist in sycamore XG.

## EXPERIMENTAL

**Enzymes.** — *Endo*-(1 $\rightarrow$ 4)- $\beta$ -D-glucanase [(1 $\rightarrow$ 4)- $\beta$ -D-glucan 4-glucanohydrolase, EC 3.2.1.4], which selectively cleaves the unbranched 4-linked glucosyl residues of XGs<sup>4</sup>, was isolated from cultures of *Trichoderma reesei*<sup>4</sup>. *Endo*- $\alpha$ -(1 $\rightarrow$ 4)-polygalacturo-



nase (poly[(1→4)- $\alpha$ -D-galacturonide]glycanohydrolase, EC 3.2.1.15) was purified to apparent homogeneity from a commercial preparation of pectin-degrading enzymes<sup>19</sup>.

*Preparation of oligosaccharide subunits of XG.* — Deacylated XG (620 mg), prepared from *endo*- $\alpha$ -(1→4)-polygalacturonase-treated SEPS as previously described, was dissolved in 310 mL of 50 mM sodium acetate buffer (pH 5.2) containing 0.02% thimerosal, and digested for 96 h at 25° with *endo*-(1→4)- $\beta$ -D-glucanase (12.4 units; one unit is defined as the amount of enzyme that releases 1  $\mu$ mole/min of reducing glucose from 1% carboxymethyl cellulose at pH 5.2 and 25°). The digestion products were passed through a column (1  $\times$  30 cm) of Dowex-50W (H<sup>+</sup>) and then through a column (1  $\times$  30 cm) of Dowex-2 (CO<sub>3</sub><sup>2+</sup>). The eluate was concentrated and lyophilized, yielding 604 mg of mixed XG oligosaccharides.

*Bio-Gel P-2 chromatography.* — XG oligosaccharides (10 or 60 mg) were applied to a column (1.6  $\times$  96 cm) of Bio-Gel P-2 (–400 mesh) and eluted with distilled water at a flow rate of 0.2 mL/min, collecting 1.3-mL fractions. The eluted oligosaccharides were monitored by differential refractometry (Waters). The amount of carbohydrate in each fraction was estimated by the anthrone assay<sup>21</sup>. The oligosaccharides with from 17 to 20 residues (shaded area, Fig. 1) were further separated by h.p.l.c.

*High-performance liquid chromatography (h.p.l.c.).* — H.p.l.c. was conducted at ambient temperature using a Waters 6000A pump system and a differential refractometer (Knauer). Oligosaccharides were applied (2 mg per injection, see Fig. 2) to an amino-bonded column (Dynamax-60A, 0.6  $\times$  27 cm, Rainin) and eluted with CH<sub>3</sub>CN:H<sub>2</sub>O in various proportions (Figs. 2 and 7) at a flow rate of 1 mL/min. The oligosaccharide-containing fractions eluted from the amino-bonded column were pooled as indicated and passed through a column (1  $\times$  30 cm) of Sephadex G-15 to remove low-molecular-weight, non-carbohydrate contaminants. Oligoglycosyl alditols were separated by reversed-phase chromatography on analytical (0.25  $\times$  25 cm) and semipreparative (1  $\times$  25 cm) octadecylsilyl silica columns (Hibar Lichrosorb RP-18, E. Merck) eluted at flow rates of 1.0 and 2.0 mL/min, respectively, with CH<sub>3</sub>OH:H<sub>2</sub>O in various proportions (see Fig. 3).

*Reduction of XG oligosaccharides.* — Oligosaccharides were dissolved (10 mg/mL) in M NH<sub>4</sub>OH containing NaBH<sub>4</sub> (10 mg/mL). After 1 h, the reaction mixture was chilled in an ice bath, and the pH was adjusted to approximately 4.9 by addition of 5M acetic acid. The products (oligoglycosyl alditols, OAs) were desalted on a column (1  $\times$  30 cm) of Sephadex G-15, concentrated to a small volume in H<sub>2</sub>O and stored at –20°.

*Chemical analyses.* — Glycosyl-residue and glycosyl-linkage compositions were determined as previously described<sup>13,22</sup>. Partially methylated alditol acetates (PMAAs) eluted from the SP2330 capillary g.l.c. column were quantitated by a modification of the selected-ion monitoring method of Waeghe *et al.*<sup>14</sup>. The structure of **6** was rigorously established in a previous study, and **6**, therefore, was used as a standard compound. The PMAA derivatives prepared from **6**–**12** were subjected to g.l.c.-m.s., and selected-ion chromatograms were generated for fragment ions that are diagnostic for each PMAA. For example, T-Araf residues were quantitated by analysis of the ion chromatogram for *m/z* 118 (see Table IV). The selected-ion chromatograms were integrated in order to

determine the (absolute) ion response for each PMAA in each sample. Relative ion response factors for each PMAA were calculated by dividing each absolute ion response obtained upon analysis of **6** by the number of residues in **6** giving rise to the PMAA in question. Thus, an estimation of the relative amount of each residue type in a particular OA was obtained by dividing the absolute ion response for each PMAA by the appropriate relative ion response factor. No 3-linked  $\beta$ -Xyl was present in **6**, and, therefore, the relative ion response factor for 3-linked Xylp was estimated by assuming that **12** contained a single 3-linked Xylp residue and a single 6-linked Xylp residue. This assumption was based on strong spectroscopic evidence (see Results and Discussion section). The relative ion response factor for 3-linked Xylp was then calculated relative to that of 6-linked Glcp, as described above. The recovery of 4-*O*-acetyl-1,2,3,4,6-penta-*O*-methyl-D-glucitol (corresponding to 4-linked glucitol) was extremely variable, due to the high volatility of this derivative.

*Fast-atom bombardment-mass spectrometry.* — F.a.b.-mass spectra were recorded with a VG Analytical ZAB-SE mass spectrometer, using 1-amino-2,3-dihydroxypropane for negative-mode spectra of underivatized OAs and thioglycerol for positive-mode spectra of per-*O*-acetylated OAs<sup>5</sup>.

*<sup>1</sup>H-N.m.r. spectroscopy.* — All samples were dissolved in deuterium oxide (99.9% <sup>2</sup>H, Aldrich) to replace exchangeable protons with deuterons and dried under a stream of dry nitrogen. Samples were then dissolved in deuterium oxide (99.96% <sup>2</sup>H, Cambridge Isotope Laboratories) and transferred to a 5-mm n.m.r. tube. <sup>1</sup>H-n.m.r. spectra were recorded as previously described<sup>5</sup> with a Bruker AM 500 n.m.r. spectrometer.

*Treatment of OAs with endo-(1→4)- $\beta$ -D-glucanase.* — OAs (100  $\mu$ g) were dissolved in sodium acetate buffer (50 mM, pH5, 850  $\mu$ L) containing endo-(1→4)- $\beta$ -D-glucanase (either 0.002 or 0.2 units) and incubated for 14 h at 30°. Addition of 0.002 U of enzyme corresponded to a ratio of enzyme to substrate that was equivalent to that used during the initial endo-(1→4)- $\beta$ -D-glucanase treatment of the polymeric XG (see above). The digested OAs were passed through a column of Dowex-50W (H<sup>+</sup>) and separated by h.p.l.c. on an amino-bonded column (Dynamax-60A, 0.6  $\times$  27 cm, Rainin). The purified oligomeric products were passed through a Sephadex G-15 column and reduced with NaBH<sub>4</sub> (see above).

#### ACKNOWLEDGMENTS

This research was supported by Department of Energy (DOE) grant DE-FG09-85ER13426 and by DOE grant DE-FG09-87ER13810 as part of the USDA/DOE/NSF Plant Science Centers program. The authors wish to thank Dr. Jerry Thomas for preparing the endo-(1→4)- $\beta$ -D-glucanase, Dr. Carl Bergmann for preparing the endo-polygalacturonase, Dr. Leszek Poppe for advice concerning the implementation of <sup>1</sup>H-n.m.r. experiments, and Dennis Warrenfeltz for maintenance of the n.m.r. and mass spectrometers and for invaluable consultation regarding their operation.

## REFERENCES

- 1 T. Hayashi, *Annu. Rev. Plant Physiol. Plant Mol. Biol.*, 40 (1989) 139–168.
- 2 W. S. York, A. G. Darvill, and P. Albersheim, *Plant Physiol.*, 75 (1984) 295–297.
- 3 G. J. McDougall and S. C. Fry, *J. Plant Physiol.*, 137 (1991) 332–336.
- 4 W. D. Bauer, K. W. Talmadge, K. Keegstra, and P. Albersheim, *Plant Physiol.*, 51 (1973) 174–187.
- 5 W. S. York, H. van Halbeek, A. G. Darvill, and P. Albersheim, *Carbohydr. Res.*, 200 (1990) 9–31.
- 6 W. S. York, J. E. Oates, H. van Halbeek, A. G. Darvill, P. Albersheim, P. R. Tiller, and A. Dell, *Carbohydr. Res.*, 173 (1988) 113–132.
- 7 L. L. Kiefer, W. S. York, P. Albersheim, and A. G. Darvill, *Carbohydr. Res.*, 197 (1990) 139–158.
- 8 B. S. Valent, A. G. Darvill, M. McNeil, B. K. Robertsen, and P. Albersheim, *Carbohydr. Res.*, 79 (1980) 165–192.
- 9 K. Koizumi, Y. Okada, U. Horiyama, T. Utamura, M. Hisamatsu, and A. Amemura, *J. Chromatogr.*, 265 (1983) 89–96.
- 10 R. Stuike-Prill and B. Meyer, *Eur. J. Biochem.*, 194 (1990) 903–919.
- 11 M. Rance, O. W. Sorensen, G. Bodenhausen, G. Wagner, R. R. Ernst, and K. Wüthrich, *Biochem. Biophys. Res. Commun.*, 117 (1983) 479–485.
- 12 S. Subramanian and A. Bax, *J. Magn. Reson.*, 71 (1987) 325–330.
- 13 S. Hakomori, *J. Biochem.*, 55 (1964) 205–208.
- 14 T. J. Waeghe, A. G. Darvill, M. McNeil, and P. Albersheim, *Carbohydr. Res.*, 123 (1983) 281–304.
- 15 W. S. York, L. L. Kiefer, P. Albersheim, and A. G. Darvill, *Carbohydr. Res.*, 208 (1990) 175–182.
- 16 A. Dell, *Adv. Carb. Chem. Biochem.*, 45 (1987) 19–72.
- 17 M. Hisamatsu, W. S. York, G. Impallomeni, A. G. Darvill, and P. Albersheim, *Carbohydr. Res.*, 211 (1991) 117–129.
- 18 J. F. G. Vliegenthart, L. Dorland, and H. van Halbeek, *Adv. Carbohydr. Chem. Biochem.*, 41 (1983) 209–374.
- 19 F. Cervone, G. De Lorenzo, L. Degra, and G. Salvi, *Plant Physiol.*, 85 (1987) 626–630.
- 20 W. S. York, A. G. Darvill, M. McNeil, T. T. Stevenson, and P. Albersheim, *Methods Enzymol.*, 118 (1985) 3–40.
- 21 Z. Dische, *Methods Carbohydr. Chem.*, (1962) 478–481.
- 22 P. Albersheim, D. J. Nevins, P. D. English, and A. Karr, *Carbohydr. Res.*, 5 (1967) 340–345.